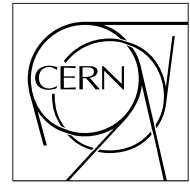


The Compact Muon Solenoid Experiment

CMS Note

Mailing address: CMS CERN, CH-1211 GENEVA 23, Switzerland



17 November 1998

Estimate of Combined Muon/Calorimeter Trigger Rates

J. Pliszka

Institute of Theoretical Physics, Warsaw University, Poland

G. Wrochna

CERN, Geneva, Switzerland

Abstract

Rates of combined muon/calorimeter triggers have been studied. The study was based on PYTHIA simulation package and a collection of subroutines for approximate, but very fast estimation of trigger response. Rates of independent muon and calorimeter triggers have been also calculated for a cross-check with detailed simulation.

As a result a set of trigger thresholds is proposed to maintain the 1st level trigger output rate at 30 kHz. The thresholds are low enough to fulfil the CMS physics program presented in the CMS Technical Proposal.

Introduction

The CMS 2nd Level Trigger is design to receive up to 100 kHz events [1]. The 1st Level is assumed to deliver not more than 30 kHz in order to ensure a safety margin. This bandwidth should be divided between muon and calorimeter triggers. Rates of calorimeter triggers, i.e. one or two electrons or photons; electron from a b-quark decay; 1, 2, 3 or 4 jets; electron/photon + jet; missing transverse energy \cancel{E}_t and total transverse energy ΣE_t , have been already calculated [2]-[12]. The muon trigger was also simulated and the rates of one and two muon trigger are known [13]-[17]. The aim of the present study is to calculate combined muon/calorimeter trigger rates, namely μ -e, μ -jet, μ - \cancel{E}_t , and μ - ΣE_t .

The study was done for the old ECAL geometry with towers of 6×6 crystals. However, we decided to publish the results because no dramatic changes in trigger rates are expected going to 5×5 towers. In any case, more detailed study should be done with more sophisticated simulation tools and the results presented here should be considered only as the first approximation.

Combined muon/calorimetric triggers have a great importance for many processes to be studied in the future pp colliders. The presence of a high energetic muon gives a very good event signature mainly due to the significant improvement in the signal/noise ratio. In case of the CMS detector in many processes it might be sufficient to use muon trigger alone but there are processes where only combined muon/calorimetric signature makes the study feasible. There are also several processes for which the combined signature is expected to improve the efficiency significantly since the muon requirement should allow for important reduction in calorimetric cut values extending in this way the physics potential. These processes are enlisted in Table 1.

Table 1: Physics channels involving combined muon/calorimeter triggers.

physics channel	μ e/ γ	μ jet	μ \cancel{E}_t
$t\bar{t}$, WZ, $W\gamma$ production	+	+	+
H, h $\rightarrow ZZ^{(*)} \rightarrow \mu\mu ee$	+		
H, h $\rightarrow ZZ^{(*)} \rightarrow \mu\mu$ 2jets		+	
H, h $\rightarrow ZZ^{(*)} \rightarrow \mu\mu \nu\nu$			+
H, h $\rightarrow WW \rightarrow \mu\nu$ 2jets		+	+
Wh, Zh, Hh $\rightarrow \ell(\ell) \gamma\gamma$	+		
h, A, H $\rightarrow \tau\tau \rightarrow e\nu\nu \mu\nu\nu$	+		+
h, A, H $\rightarrow \tau\tau \rightarrow \ell\nu\nu$ had.	+	+	+
$t\bar{t} \rightarrow H^\pm b Wb$	+	+	+
$H^\pm \rightarrow \tau\nu$; $W \rightarrow \ell\nu$	+	+	+
$B_d^0 \rightarrow J/\psi K_s^0$ $b_{tag} \rightarrow \mu$ or e + control channels	+		
$B_d^0 \rightarrow \pi^+ \pi^-$ $b_{tag} \rightarrow \mu$ or e		+	
$B_s^0 \rightarrow D_s \pi \rightarrow \varphi \pi \pi \rightarrow KK \pi\pi$ $b_{tag} \rightarrow \mu$ or e		+	
$\tilde{g}\tilde{g}, \tilde{q}\tilde{q} \rightarrow 1-4 \ell \chi_1^0 + X$	+	+	+
$\tilde{\ell}\tilde{\ell} \rightarrow 2-3 \ell \chi_1^0$'s	+		+
$\chi_2^0 \chi_1^\pm \rightarrow \ell\ell \chi_1^0 \ell'\nu \chi_1^0$	+		+
leptoquarks	+	+	
technicolor ρ_T, ω_T	+		

1 Simulation

The main difficulty of this study comes from a huge statistics needed to calculate trigger rates. In order to accomplish the study in a limited amount of CPU time several ideas have been exploited. Among them are:

- events generation in \hat{p}_t bins,
- repeated fragmentation of the event skeleton,
- early rejection of non relevant particles and events,
- custom (non-GEANT) particle tracking and decays,
- fast (non-GEANT) simulation of the calorimeter response with parametrised showers,
- parametrisation of the muon trigger response.

Here we describe them only briefly and we refer the reader to the software description in Ref. [18].

The software consists of the following parts:

- event generation,
- particle tracking and decays in the detector,
- simulation of the detector response,
- simulation of the trigger algorithms,
- final analysis.

1.1 Event generation

Events were generated using PYTHIA 5.7. Default parameters were taken where possible. Since the trigger rates are dominated by minimum bias events¹⁾ the main effort was put on the simulation of this process. Hard jets were simulated together with a soft background selecting option MSEL=1. In order to collect enough statistics for hard collisions the events were generated in several bins of parton transverse momentum \hat{p}_t (see Tab. 1.1). In the final analysis each bin was weighted with a cross section given by PYTHIA. Separate samples were generated for the combined muon/calorimeter triggers and for the calorimeter triggers. The later one was used to cross-check the results with previous studies.

Table 2: Generated samples. Notation “25 000×10” means that 25 000 event skeletons were generated and each one was fragmented 10 times (see text).

\hat{p}_t (GeV)	σ (mb)	calo events	muon/calor events
5-10 GeV	39.6	2 500	25 000×10
10-20 GeV	5.4	10 000	25 000×10
20-50 GeV	0.59	12 500	25 000×10
50-100 GeV	0.021	2 500	25 000×10
> 100 GeV	0.0014	2 500	25 000×10

Simulation of the muon/calor sample is especially time consuming, because only $\sim 1/1000$ of minimum bias events contains a muon which could be detected. The most time consuming part of the PYTHIA event generation is the generation of a quark-gluon skeleton. Therefore one can save a lot of CPU time repeating several times fragmentation and decays for each quark-gluon skeleton. For the purpose of muon trigger study one can repeat it 100 times without introducing a significant bias. Unfortunately in the case of combined triggers correlations between the events obtained from the same skeleton are larger because the selection is based also on the calorimeter response which is supposed not to be very dependent on the fragmentation stage. We found that in this case about 10 repetitions is an optimum.

1.2 Particle tracking and decays in the detector

In principle PYTHIA can perform all particle decays. However, long living particles like π^\pm , K^\pm , K_L^0 can travel several meters before they decay. Therefore one has to take into account possible bending in a magnetic field and interactions with detector material. To perform this task we developed a dedicated software package TRACK_AND_DECAY. It was responsible for the tracking from the surface of a cylinder with 10 cm radius and 20 cm length to the inner surface of the electromagnetic calorimeter. Decays in the small cylinder, where the influence of the magnetic field can be neglected, were left to PYTHIA.

¹⁾ Except the 2μ trigger above $p_t = 25$ GeV, where the dominant source of muons is $Z \rightarrow \mu\mu$ [17].

Due to the CPU time consumption it is very important to reject on the earliest possible stage events which are very improbable to give a trigger. Since calculation of the possible response of the calorimetric trigger is very time consuming, first the simple geometrical acceptance for muons was checked. Only events with muons with p_t over 1 GeV and $|\eta| < 2.4$ were selected for further processing, namely for simulating the calorimeter trigger response. Obviously this condition was not required for the calorimeter trigger sample.

1.3 Calorimeter trigger simulation

1.3.1 Calorimeter response

Calorimeter trigger is based on three kind of detectors: electromagnetic calorimeter ECAL ($|\eta| < 3.0$), hadronic calorimeter HCAL ($|\eta| < 3.0$), and very forward calorimeter VFCAL ($2.6 < |\eta| < 5.0$). The present study are done for $|\eta| < 2.6$ and therefore the VFCAL is not used.

HCAL readout is arranged in towers of $\Delta\eta \times \Delta\phi = 0.087 \times 0.087$. This size defines *calorimeter trigger cell*.

ECAL is made out of PbWO_4 crystals. Each crystal in the barrel has a size of $\Delta\eta \times \Delta\phi = 0.0145 \times 0.0145$, thus each trigger cell contains 6×6 crystals (see Fig. 1). Each cell is divided into 6 *strips* of $\Delta\eta \times \Delta\phi = 0.0145 \times 0.087$ i.e. 1×6 crystals. In the endcaps the number of crystals per cell depends on pseudorapidity.

The calorimeter response was obtained with modified CALTRIG package [19]. The energy of each particle entering calorimeters was deposited in the ECAL and HCAL cells. For this purpose a realistic geometry of the cells and parametrisations of electromagnetic and hadronic showers was used. A stochastic noise was added to each cell and the digitisation was applied. It consists of cutting the signals which are below the threshold ($= 3 \sigma_{noise}$) and rounding the energy values to multiples of 0.5 or 1.0 GeV (see Tab. 3).

Table 3: Parameters of the calorimeter simulation.

ECAL noise (raw energy)	$\sigma_{noise}^E = 0.025$ GeV per crystal
HCAL noise (raw energy)	$\sigma_{noise}^H = 0.25$ GeV per tower
ECAL threshold (raw energy)	$3 \sigma_{noise}^E$
HCAL threshold (raw energy)	$3 \sigma_{noise}^H$
ECAL calibration	1.0
HCAL calibration	1.0
ECAL cell digitisation step (transverse energy)	0.5 GeV
HCAL cell digitisation step (transverse energy)	0.5 GeV
ECAL+HCAL cell digitisation step (transverse energy)	1.0 GeV

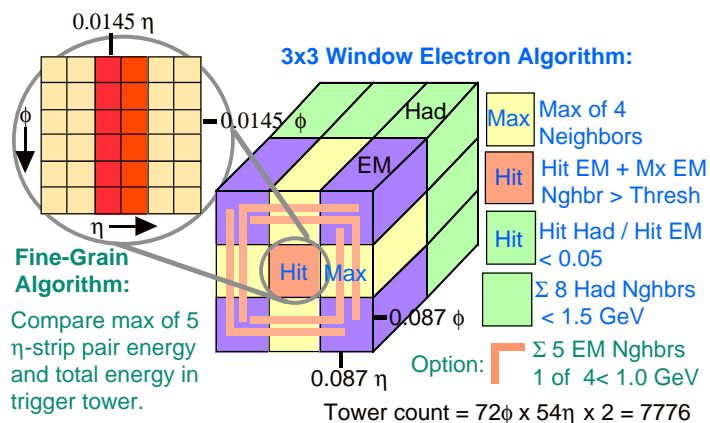


Figure 1: Calorimeter trigger primitives and cuts

1.3.2 Calorimeter trigger algorithm

The calorimeter trigger software used in this study is based on the code used in the CMSIM package [20]. Modifications, which were mainly of technical nature, are described in [18]. Here we just briefly summarise simulated trigger algorithms. Detailed description of the algorithms can be found in [22].

Trigger primitives. The following *trigger primitives* are generated by the calorimeter front-end electronics:

- transverse energy E_t inside an ECAL cell,
- fine grain local isolation bit LI,
- transverse energy H_t inside an HCAL cell,
- MIP bit – energy deposit compatible with minimum ionising particle.

The LI bit for each cell is computed in the following way. For each pair i of adjacent strips in the 6×6 ECAL cell a sum L_t^i of transverse energy deposits is calculated. The largest one L_t^{max} is found. The ratio $R = L_t^{max}/E_t$ is compared to a programmable threshold R^{thres} . If $R > R^{thres}$ the LI bit is set. The trigger primitives are used as a basic information for all the calorimeter triggers.

Electron/photon trigger. Let us introduce the following symbols for calorimeter cells and transverse energy deposited in them (see Fig. 1):

- E_t^{hit} — the ECAL cell containing most of the energy
- E_t^{max} — cell with maximal E_t of four E_t^{hit} neighbours
- H_t^{hit} — the HCAL cell behind the E_t^{hit}
- Σ_8^H — sum of H_t of 8 cells around H_t^{hit}
- Σ_5^E — sum of E_t of 5 cells (L-shaped "corner") around E_t^{hit}
- E_t^{thres} — the electron/photon threshold

An electron/photon candidate has to fulfil requirements listed in Tab. 4. Different sets of thresholds were used for low and high luminosity, as suggested in Ref. [6].

Table 4: Electron/photon trigger cuts.

observable	symbol	cut for $\mathcal{L} = 10^{33} \text{cm}^{-2} \text{s}^{-1}$	cut for $\mathcal{L} = 10^{34} \text{cm}^{-2} \text{s}^{-1}$
lateral shower profile	$R = L_t^{max}/E_t^{hit}$	< 0.89	< 0.89
longitudinal shower profile	H_t^{hit}/E_t^{hit}	< 0.04	< 0.07
hadronic isolation	Σ_8^H	$< 0.5 \text{ GeV}$	$< 2.2 \text{ GeV}$
electromagnetic isolation	At least one of four Σ_5^E	$< 1.2 \text{ GeV}$	$< 2.0 \text{ GeV}$
transverse energy threshold	$E_t^{hit} + E_t^{max} > E_t^{thres}$	variable	

The b-electron trigger. In order to reduce the E_t^{thres} for electrons from b-quark decays an additional requirement should be imposed. One can make use of the fact that a b-electron is slightly separated from the remnants of other decay products. This kind of isolation can be achieved by tightening the cut on the R parameter. Normal hadronic and electromagnetic isolation should not be, however used. The full list of the b-electron cuts is given in Tab. 1.3.2.

Table 5: The b-electron trigger cuts (used at $\mathcal{L} = 10^{33} \text{cm}^{-2} \text{s}^{-1}$ only).

observable	symbol	cut
lateral shower profile	$R = L_t^{max}/E_t^{hit}$	< 0.95
longitudinal shower profile	H_t^{hit}/E_t^{hit}	< 0.05
hadronic isolation		not used
electromagnetic isolation		not used
transverse energy threshold	$E_t^{hit} + E_t^{max} > E_t^{thres}$	variable

Jet triggers. For the purpose of jet triggers the jet transverse energy E_t^{jet} was defined as a sum of the transverse energies $E_t + H_t$ computed in a certain calorimeter region (4×4 cells). It was used as a threshold for single- and multijet triggers. In the case of multijet triggers a separation of minimum one cell between two jet candidates was required.

Missing and total E_t trigger. These triggers also use the sum of the transverse energies $E_t + H_t$ computed in calorimeter regions (4×4 cells). The missing energy \cancel{E}_t is a vector and the total energy ΣE_t is a scalar sum of the values for all regions. \cancel{E}_t and ΣE_t were used as thresholds for the respective triggers.

1.3.3 Comparison with detailed simulation

The results of the analysis of the calo sample were compared to the results of the detailed simulation done with the CMSIM package, based on GEANT. They are presented in Figures 2-6.

In the case of electron/photon and b-electron triggers the comparison is shown after each cut. The agreement between the fast and detailed simulation after all cuts is satisfactory. The e/γ rate at low E_t is slightly overestimated which means that our conclusions will be rather conservative.

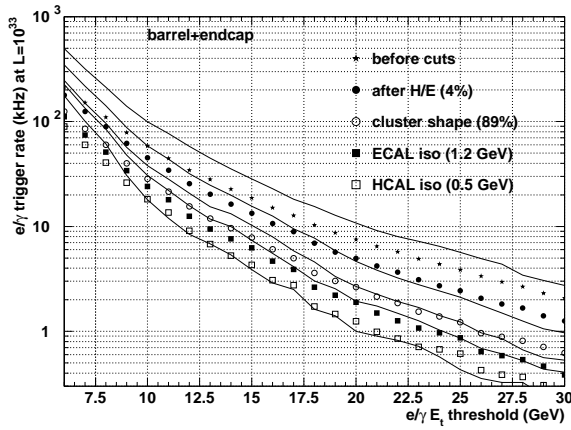


Figure 2: Electron/photon trigger rate. Curves — fast simulation (this study), points — detailed simulation [6].

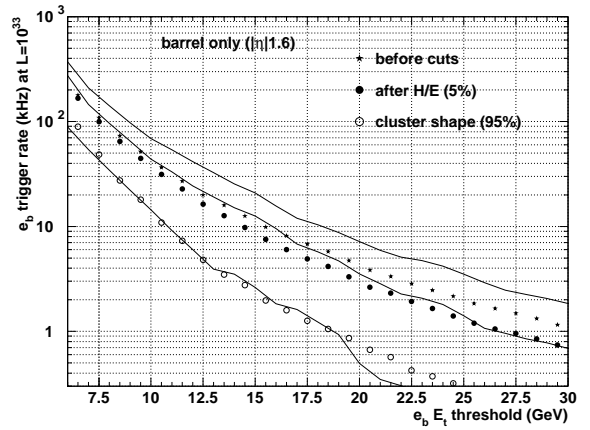


Figure 3: The b-electron trigger rate. Curves — fast simulation (this study), points — detailed simulation [5].

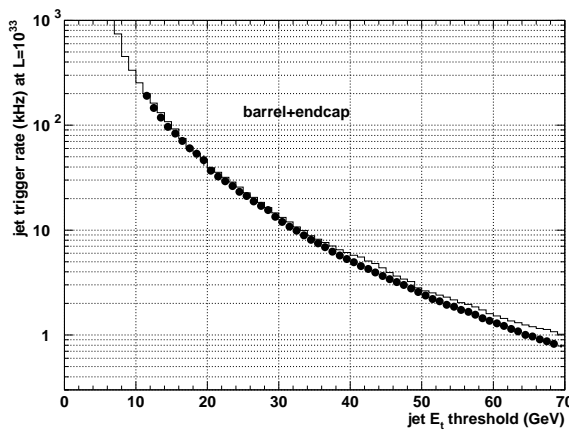


Figure 4: Jet trigger rate. Histogram — fast simulation (this study), points — detailed simulation [23].

The agreement of jet trigger rate shown in Fig. 4 is impressive. The missing energy \cancel{E}_t is overestimated as much as factor 2. Being a vector sum this quantity is the most sensitive to the geometrical details and one should not expect that the simple simulation can reproduce it well. Our result we can consider, however, as an upper limit of the expected \cancel{E}_t trigger rate.

In the case of the ΣE_t trigger only one point from the detailed simulation was available. The agreement at this point is very good.

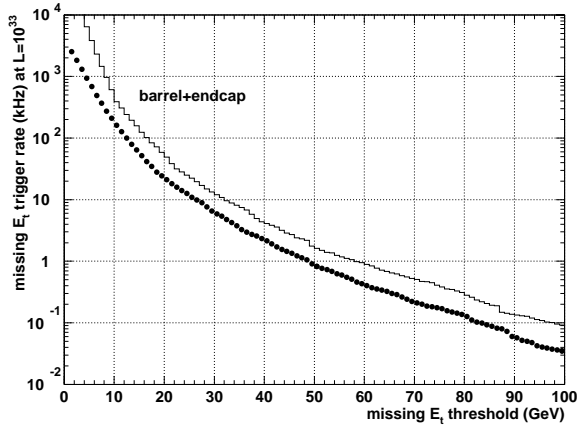


Figure 5: \cancel{E}_t trigger rate. Histogram — fast simulation (this study), points — detailed simulation [12].

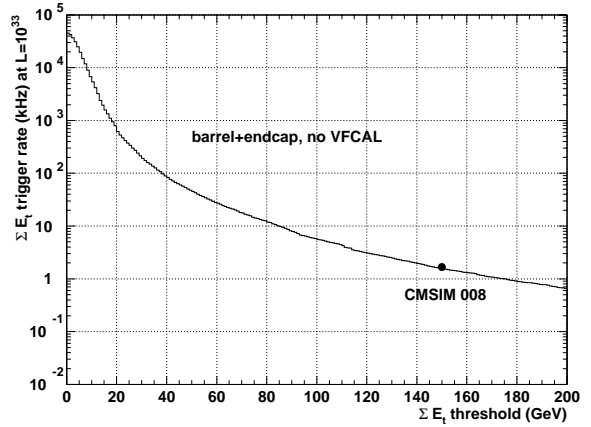


Figure 6: ΣE_t trigger rate. Histogram — fast simulation (this study), point — detailed simulation [23].

1.4 Muon trigger simulation

1.4.1 Simulation software

In order to save CPU time we did not simulate explicitly muon tracks, muon detector response and trigger algorithms. Instead we used slightly modified version of the parametrisation EFFMRPC described in [21]. It gives the response of the *Pattern Comparator Trigger* (PACT) which compares each pattern of hit RPC strips to predefined patterns corresponding to various p_t . The algorithm is described in details elsewhere [24].

1.4.2 Comparison with detailed simulation

One and two muon trigger rates obtained in this study are compared to the results of detailed simulation in Figures 7 and 8 respectively. The detailed simulation [17] was done with the CMSIM package. The agreement is satisfactory.

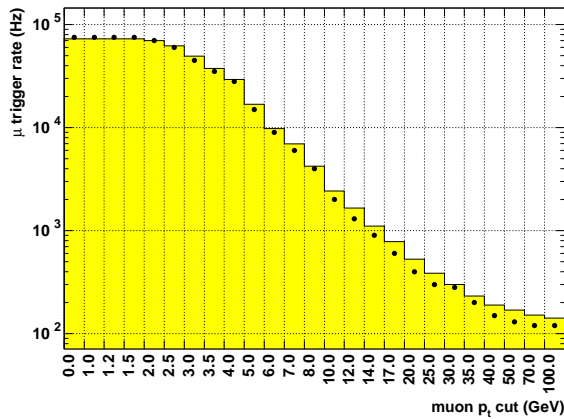


Figure 7: Single muon trigger rate at $\mathcal{L} = 10^{33} \text{cm}^{-2} \text{s}^{-1}$. Histogram — fast simulation (this study), points — detailed simulation [17].

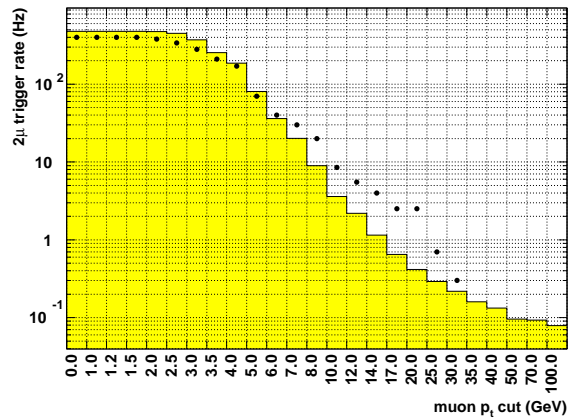


Figure 8: Two muon trigger rate at $\mathcal{L} = 10^{33} \text{cm}^{-2} \text{s}^{-1}$. Histogram — fast simulation (this study), points — detailed simulation [17].

2 Results

Obtained trigger rates are presented in Tables 6-12. Each table cell contains the trigger rate (in 100 Hz units) for objects with p_t or E_t above the given thresholds.

Table 6: Two muon trigger rate in 100 Hz units at $\mathcal{L} = 10^{33} \text{cm}^{-2} \text{s}^{-1}$ as a function of p_t cuts on the two muons.

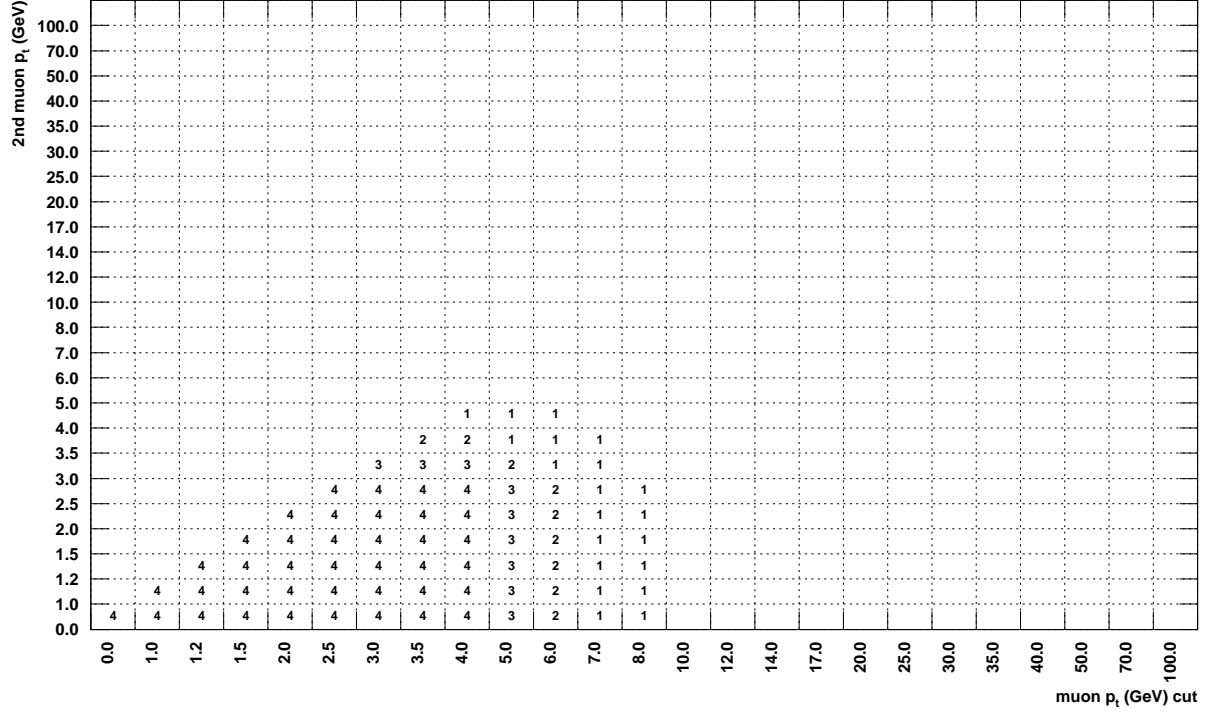


Table 7: Cumulative single- and two-muon trigger rate in 100 Hz units at $\mathcal{L} = 10^{33} \text{cm}^{-2} \text{s}^{-1}$ as a function of the p_t cuts. The two-muon p_t cut is the same for both muons.

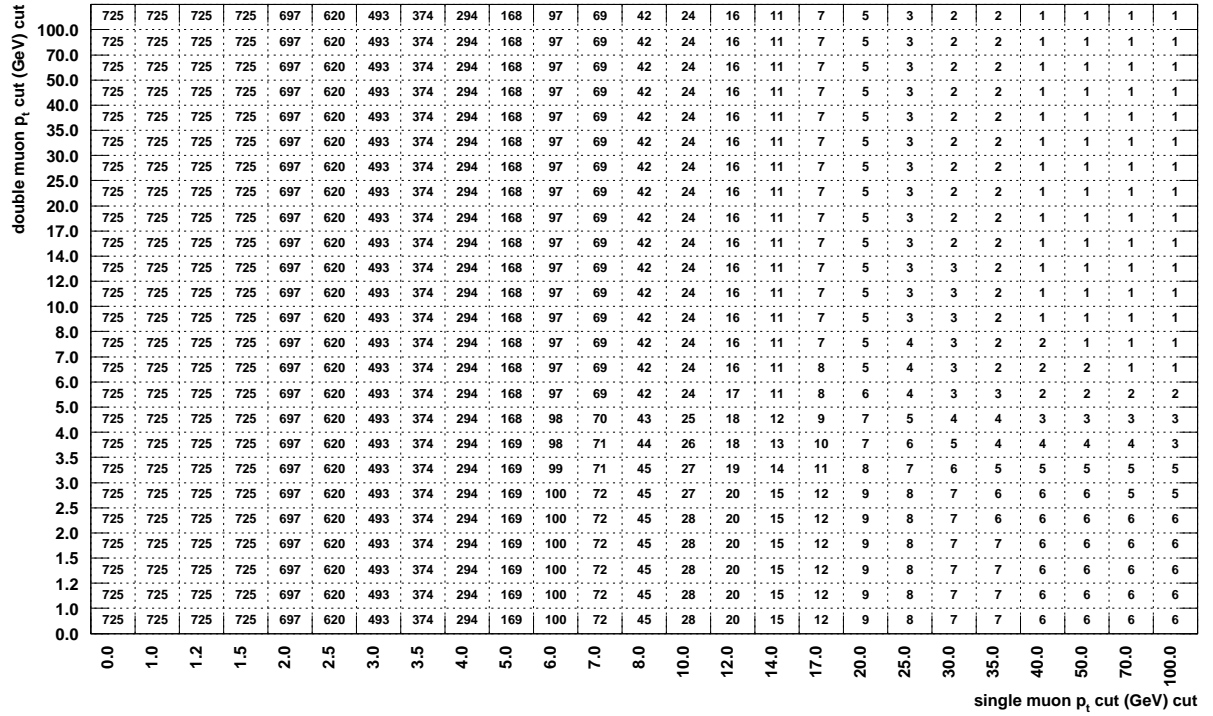


Table 12: Muon- ΣE_t trigger rate in 100 Hz units at $\mathcal{L} = 10^{33} \text{cm}^{-2} \text{s}^{-1}$.

total E_t (GeV) cut	0.0	1.0	1.2	1.5	2.0	2.5	3.0	3.5	4.0	5.0	6.0	7.0	8.0	10.0	12.0	14.0	17.0	20.0	25.0	30.0	35.0	40.0	50.0	70.0	100.0
480.0																									
460.0																									
440.0																									
420.0																									
400.0																									
380.0																									
360.0																									
340.0																									
320.0																									
300.0																									
280.0																									
260.0																									
240.0	1	1	1	1	1	1																			
220.0	1	1	1	1	1	1	1	1	1	1															
200.0	1	1	1	1	1	1	1	1	1	1	1														
180.0	2	2	2	2	2	1	1	1	1	1															
160.0	2	2	2	2	2	2	2	2	2	1	1	1													
140.0	3	3	3	3	3	3	3	2	2	1	1	1	1												
120.0	5	5	5	5	5	4	4	3	3	2	2	1	1	1											
100.0	6	6	6	6	6	5	5	4	3	2	2	1	1	1											
80.0	13	13	13	13	13	11	10	9	7	6	5	4	2	1	1										
60.0	25	25	25	25	24	23	21	19	17	11	9	7	5	3	2	1	1								
40.0	56	56	56	56	55	50	45	40	34	21	16	13	10	5	3	2	2	1	1						
20.0	193	193	193	193	188	172	143	111	90	54	35	27	18	9	7	5	3	2	1	1	1	1	1	1	1
0.0	725	725	725	725	697	620	493	374	294	168	97	69	42	24	16	11	7	5	3	2	2	1	1	1	1

In the case of two-object triggers at low luminosity we can afford the lowest possible muon p_t cut. It is determined by the muon energy loss in the calorimeters and therefore it varies with η . In the barrel it is ≈ 4 GeV. In the endcaps it decreases down to ≈ 2 GeV at $|\eta| = 2.4$. More precisely one can define the threshold as:

$$\begin{aligned}
 p_t &> 4.0 \text{ GeV} && \text{for } |\eta| < 1.5 \\
 p_t &> 2.5 \text{ GeV} && \text{for } 1.5 < |\eta| < 1.9 \\
 p_t &> 2.0 \text{ GeV} && \text{for } 1.9 < |\eta| < 2.4
 \end{aligned}$$

At high luminosity it is convenient to set the muon threshold for two-object triggers at 4 GeV in the entire η range. Once we fixed the muon thresholds we can plot the two-object trigger rates as a function of the threshold on the second object. This is done in Figures 9-13.

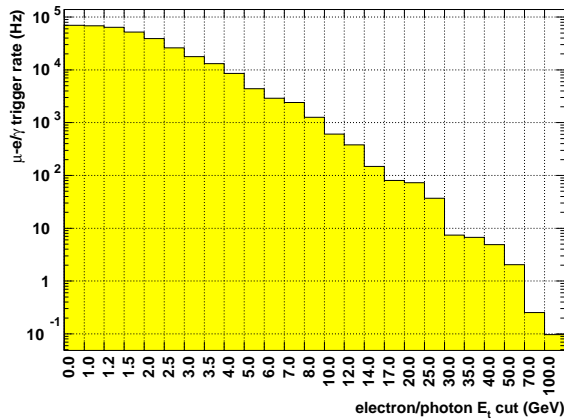


Figure 9: Muon-electron/photon trigger rate for $p_t^{cut}(\mu) = 2\text{-}4$ GeV at $\mathcal{L} = 10^{33} \text{cm}^{-2} \text{s}^{-1}$.

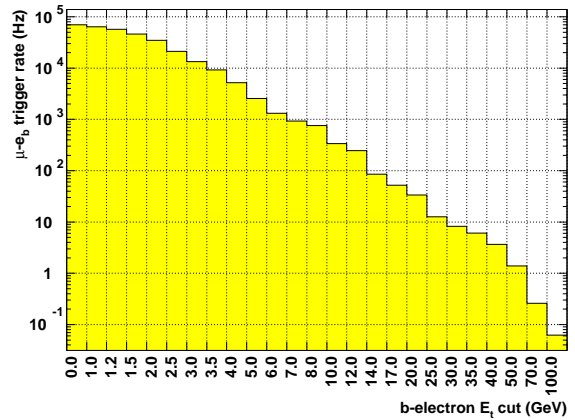


Figure 10: Muon-beauty electron trigger rate for $p_t^{cut}(\mu) = 2\text{-}4$ GeV at $\mathcal{L} = 10^{33} \text{cm}^{-2} \text{s}^{-1}$.

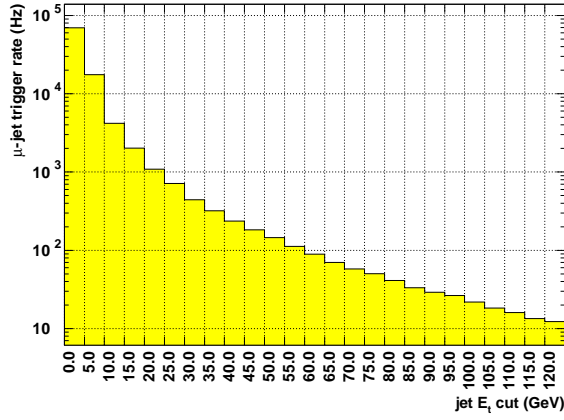


Figure 11: Muon-jet trigger rate for $p_t^{cut}(\mu) = 2-4$ GeV at $\mathcal{L} = 10^{33} \text{cm}^{-2} \text{s}^{-1}$.

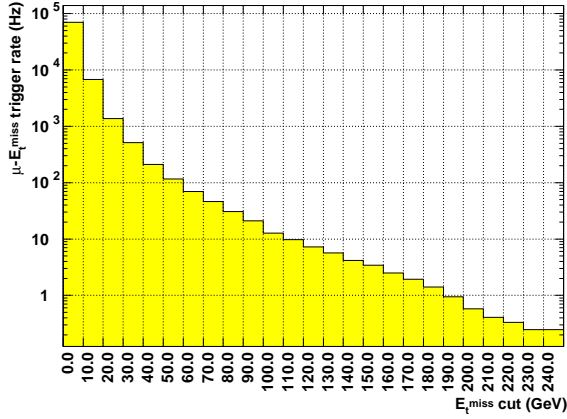


Figure 12: Muon- E_t trigger rate for $p_t^{cut}(\mu) = 2-4$ GeV at $\mathcal{L} = 10^{33} \text{cm}^{-2} \text{s}^{-1}$.

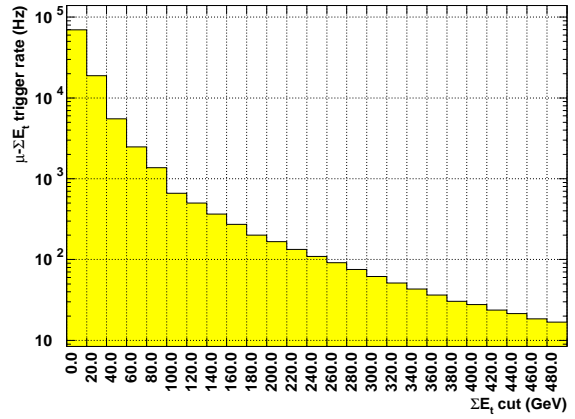


Figure 13: Muon- ΣE_t trigger rate for $p_t^{cut}(\mu) = 2-4$ GeV at $\mathcal{L} = 10^{33} \text{cm}^{-2} \text{s}^{-1}$.

All the results are summarised in Tables 13. Here we have chosen the threshold to keep the total trigger rate at 30 kHz. The rates of calorimeter triggers are taken from [10]. The case of DAQ limited to 75 kHz, i.e. the total trigger rate of 25 kHz, is presented in Table 14.

3 Conclusions

Presented muon/calorimeter trigger study accomplishes the task of calculating the 1st level trigger output rates. A set of trigger thresholds is proposed to maintain the 1st level output rate at 30 kHz. The thresholds are low enough to fulfil the CMS physics program presented in the CMS Technical Proposal [1].

The results indicate a possibility of important gain in several physics channels, especially in CP violation studies:

- CP violation — angle β : $B_d^0 \rightarrow J/\psi K_s^0$; $J/\psi \rightarrow \mu\mu$ or ee ; $b_{tag} \rightarrow \mu$ or e
 μ -e trigger — $p_t(\mu) > 2-4$ GeV; $p_t(e) > 4$ GeV
- CP violation — angle α : $B_d^0 \rightarrow \pi^+\pi^-$; $b_{tag} \rightarrow \mu$ or e
 μ -jet trigger, where the $\pi^+\pi^-$ pair is treated as a “jet” — $p_t(\mu) > 2-4$ GeV; $E_t(\pi^+\pi^-) > 10$ GeV
- CP violation — oscillations: $B_s^0 \rightarrow D_s\pi \rightarrow \varphi\pi\pi \rightarrow KK\pi\pi$; $b_{tag} \rightarrow \mu$ or e
 μ -jet trigger, where the $\pi\pi$ pair is treated as a “jet” — $p_t(\mu) > 2-4$ GeV; $E_t(\pi\pi) > 10$ GeV

Presented trigger thresholds should not be blindly used in physics simulation. They should rather be considered as examples chosen to demonstrate trigger capabilities. One should also keep in mind that the results were obtained with fast simulation program and they should be checked later by more detailed (full GEANT/CMSIM) simulations.

Table 13: Trigger rates for selected cuts. LV2 input rate = 100 kHz.

trigger type	$\mathcal{L} = 10^{33} \text{cm}^{-2} \text{s}^{-1}$			$\mathcal{L} = 10^{34} \text{cm}^{-2} \text{s}^{-1}$		
	thresholds (GeV)	rate (kHz)		thresholds (GeV)	rate (kHz)	
		individual	cumulative		individual	cumulative
ΣE_t	150	1.04	1.04	400	0.48	0.48
\cancel{E}_t	40	2.11	2.82	80	1.29	1.70
e	12	10.3	12.3	25	6.84	8.34
ee	7	1.54	13.1	12	1.45	9.52
j	50	1.98	13.5	100	2.06	10.7
jj	30	1.63	13.9	60	2.17	11.6
jjj	20	1.02	14.1	30	3.16	13.3
jjjj	15	0.68	14.2	20	2.96	14.3
ej	9 15	5.98	15.2	12 50	1.35	14.9
μ	7	7.0	7.0	20	7.8	7.8
$\mu\mu$	2-4	0.5	7.3	4	1.6	9.2
μe	2-4 7	2.4	9.2	4 8	5.5	14.4
μe_b	2-4 4	5.2	12.8			
μj	2-4 10	4.2	14.4	4 40	0.3	14.4
$\mu \cancel{E}_t$	2-4 40	0.2	14.4	4 60	1.0	15.3
$\mu \Sigma E_t$	2-4 100	0.7	14.4	4 250	0.2	15.3

Table 14: Trigger rates for selected cuts. LV2 input rate = 75 kHz.

trigger type	$\mathcal{L} = 10^{33} \text{cm}^{-2} \text{s}^{-1}$		
	thresholds (GeV)	rate (kHz)	
		individual	cumulative
μ	7	7.0	7.0
$\mu\mu$	2-4	0.5	7.3
μe	2-4 7	2.4	9.2
μe_b	2-4 4.5	3.3	11.1
μj	2-4 15	2.0	11.9
$\mu \cancel{E}_t$	2-4 40	0.2	11.9
$\mu \Sigma E_t$	2-4 100	0.7	11.9

The importance of the presented results is two-fold. General consistency of the trigger strategy and CMS physics program was demonstrated. Areas of possible improvement were identified which should be studied now with more detailed, dedicated simulation.

Acknowledgements

The authors would like to thank Marcin Konecki for providing EFFMRPC parametrisation code and useful discussions. We are grateful to Andrzej Fengler for several ideas of software improvement and speeding up the simulation. Many thanks to Ricardo Nobrega for providing the calorimeter trigger code, to Alexander Nikitenko for many important comments on the fast calorimeter simulation and to Carmen Albajar for explaining the usage of CALTRIG package. We also thanks warmly Daniel Denegri, Jan Królikowski and João Varela for many fruitful discussions.

References

- [1] *The Compact Muon Solenoid — Technical Proposal*, **CERN/LHCC 94-38**.
- [2] **CMS TN/94-219**, Ph. Busson, J. Varela, *Calorimeter Trigger in CMS Algorithm studies I*.
- [3] **CMS TN/95-027**, C. Lourenco, J. Varela, *A fine granularity calorimeter trigger for CMS*.
- [4] **CMS TN/95-143**, J. Varela, *Requirements for a fine grained calorimeter trigger*, presented at the *First Workshop on Electronics for LHC Experiments*, Lisbon, 11-15 September 1995.
- [5] **CMS TN/95-197**, C. Lourenco, A. Nikitenko, J. Varela, *A low p_t 1st level single electron trigger for beauty studies in CMS*.
- [6] **CMS TN/96-021**, R. Nobrega, J. Varela, *The CMS electron/photon trigger: simulation study with CMSIM data*.
- [7] **CMS TN/94-285**, S. Dasu, J. Lackey, W.H. Smith, W. Temple, *CMS Level 1 Calorimeter Trigger Performance Studies*.
- [8] **CMS TN/95-111**, S. Dasu, J. Lackey, W.H. Smith, W. Temple, *CMS Missing Transverse Energy Trigger Studies*.
- [9] **CMS TN/95-112**, S. Dasu, J. Lackey, W.H. Smith, W. Temple, *New Algorithms for CMS Electron/Photon Trigger — Use of Fine Grain Calorimeter Data*.
- [10] **CMS TN/95-183**, S. Dasu, J. Lackey, W.H. Smith, W. Temple, *CMS Level 1 Calorimeter Trigger Performance on Technical Proposal Physics*.
- [11] **CMS TN/96-066**, S. Dasu, W.H. Smith, *CMS Level-1 Jet Trigger Study*.
- [12] S. Dasu, C. Lourenco, A. Nikitenko, R. Nobrega, W.H. Smith, J. Varela, *Simulation of the CMS Level-1 Calorimeter Trigger*, presented at the *VI International Conference on Calorimetry in High Energy Physics*, Frascati, Italy, June 1996.
- [13] **CMS TN/92-039**, M. Konecki, J. Królikowski, G. Wrochna, *Simulation study of the RPC based, single muon trigger for CMS*.
- [14] **CMS TN/94-138**, M. Huhtinen, G. Wrochna, *Estimation of the RPC muon trigger rates due to neutral particles*.
- [15] **CMS TN/94-282**, A. Csilling, M. Konecki, J. Królikowski, G. Wrochna, *Muon Trigger Rates*.
- [16] **CMS TN/95-150**, M. Ćwiok, G. Wrochna, *Muon rates in UA1, D0, CDF and CMS predicted by PYTHIA 5.7*.
- [17] A. Fengler, *Double muon trigger rates in CMS experiment*, PHD thesis, Warsaw University, 1996, <http://cmsdoc.cern.ch/~fengler/MSc/trig2mu.ps.Z>
- [18] J. Pliszka, G. Wrochna, *Fast simulation tools for trigger study*, talk given at the CMS Software Week, CERN, October 1996, http://cmsdoc.cern.ch/~wrochna/GW_talks/trackdec.ps
- [19] A. Nikitenko, presented at the *CMS Calorimeter Trigger Meeting*, 17 February 1997. Some information can be found in **CMS TN/94-187**, A. Nikitenko, *Towards the fast hadron Monte Carlo for CMS calorimetry*.
- [20] *CMS Simulation Package — Users' Guide and Reference Manual*, <http://cmsdoc.cern.ch/cmsim/cmsim.html>
- [21] **CMS TN/96-104**, M. Konecki, J. Królikowski, G. Wrochna, *Parametrisation functions of the RPC based muon trigger*.
- [22] **CMS TN/96-10**, *CMS Calorimeter Trigger — Preliminary specifications of the baseline trigger algorithms.*
- [23] A. Nikitenko, private communication.
- [24] **CMS TN/96-60**, *CMS Muon Trigger — Preliminary specifications of the baseline trigger algorithms*.